Journal of Alloys and Compounds 780 (2019) 170–176

Contents lists available at ScienceDirect

Journal of Alloys and Compounds

journal homepage: http://www.elsevier.com/locate/jalcom

Synthesis, characterization and electrochemical properties of the layered high capacity sodium ion intercalation cathode material

Yu Wang, Xianyou Wang*, Ruizhi Yu, Xiaohui Zhang, Manfang Chen, Ke Tang, Yan Huang

National Base for International Science & Technology Cooperation, National Local Joint Engineering Laboratory for Key Materials of New Energy Storage Battery, Hunan Province Key Laboratory of Electrochemical Energy Storage & Conversion, School of Chemistry, Xiangtan University, Xiangtan 411105, Hunan, China

Article history:
Received 9 August 2018
Received in revised form
18 November 2018
Accepted 28 November 2018
Available online 29 November 2018

Keywords:
Sodium ion batteries
Cathode materials
Layered oxides
$NaMn_{2/3}Ni_{1/6}Co_{1/6}O_2$
Phase transitions
Electrochemical performances

Because of the high safety, abundant resource and low cost of sodium ion batteries (SIBs), lithium ion batteries (LIBs) will be replaced by SIBs with the ever-increasing market demand for high performance and low cost energy storage battery system. However, the short cycle life and poor rate performance for current SIBs restrict their further application. Cathode materials are the most important component for the development of SIBs, which have an unparalleled effect on enhancing the electrochemical performance of SIBs. Herein, a high electrochemical performance O3-type $NaMn_{2/3}Co_{1/6}Ni_{1/6}O_2$ is synthesized by hydrothermal method and high-temperature annealing. The as-prepared sample shows the uniform spherical morphology and exhibits a specific capacity of 153.6 mAh g^{-1} with high capacity retention of 81.7% after 100 cycles and the coulombic efficiency of 98%. Moreover, the sample also exhibits excellent rate performance and the reversible capacity is 91.6 mAh g^{-1} at 1 C. The remarkably enhancing electrochemical performances make it be considered as a promising cathode active material of SIBs.

© 2018 Elsevier B.V. All rights reserved.

1. Introduction

As the global energy crisis worsens, finding clean and sustainable new energy is imperative in contemporary society. At the same time, energy production and storage technologies are increasingly concerned with the rapid development of solar and wind energy technology. Among all various electrical energy storage (EES) technologies, rechargeable batteries are considered as the most commercially viable energy storage technology [1]. As the most suitable power source for portable electronic products, LIBs have received the most widely concerned and research as rechargeable batterie. However, with the large-scale commercial application of LIBs, their disadvantages such as insufficient resources and high costs are gradually exposed. Simultaneously, the advantages of SIBs, such as high safety and sustainability, prompt researchers to use Na^+ to assemble SIB because SIBs have the similar storage mechanism of LIBs [2]. As well as sodium electropositive nature is closer to lithium [3,4], making it become a promising alternative for the development of the next generation of energy storage devices [5]. In addition, Na is more rich in natural abundant (2.64 wt % abundance on Earth) and cheaper than Li [6], therefore SIBs become more prospective energy storage system as a large-scale grid energy storage devices [7].

As we all know, the exploration of SIBs began in the early 1980s [8,9]. During a long period of academic research, the positive electrode is the key factor for restricting the high electrochemical performance of SIBs [10]. The collapse of the structure of the SIBs cathode materials will be occurred during Na^+ intercalation/deintercalation since Na has a larger ionic radius than Li (0.076 vs. 0.102 nm [11]. Therefore, SIBs cathode materials exhibit a poor rate capacity and cycle performance, thus limiting the application of SIBs. Therefore, there is an urgent demand to develop the high electrochemical performance cathode materials of SIBs. During the recent researches on the cathode materials, various functional materials have been proposed and used as cathode materials, including transition-metal oxides, polyanionic compounds, metal hexacyanometalates and organic compounds [12]. Among all materials, transition-metal oxides that are described as Na_xMO_2 (M = Mn, Co, Ni, Fe, etc.) have attracted wide interest as due to the flexibility and versatility of transition-metal oxides [13], and are considered as a kind of promising cathode material for SIBs.

According to the cationic distributions, transition-metal oxides are usually divided into two main categories: layered-Na_xMO_2 and

* Corresponding author.
E-mail address: wxianyou@yahoo.com (X. Wang).

https://doi.org/10.1016/j.jallcom.2018.11.369
0925-8388/© 2018 Elsevier B.V. All rights reserved.

tunnel-$NaMO_2$ [12]. Because of the larger screening effect, sodium has a strong tendency to favor the formation of layered compounds [14]. Therefore, the layered oxides are in dominant proportions in various transition-metal oxides. According to the arrangement of the sodium layer and the transition-metal, layer metal oxides can be classified into two most-common structural polymorphs: P2-phase (Na layers and transition-metal (M) layers stacked in the ABBAABBA manner in which Na^+ and transition-metal ions are individually located in the octahedral sites) and O3-phase (Na layers and transition-metal (M) layers packed closely in the ABCABC pattern, and the Na^+ are all located in the trigonal prismatic sites of the Na layers). When the x values of 0.83—1.0 is the electroactive O3-phase and the x values of 0.67—0.80 is P2-phase [15,16]. Both the P2-Phase and O3-phase can be easily synthesized by co-precipitation reactions, solid-state routes, and hydrothermal methods in air [17—19]. Compared with layered P2 oxides, layered O3 oxides can provide sufficient Na^+ in cells and show higher ion-diffusion coefficients which have been considered as a promising high-energy cathode material of SIB [20]. For instance, as reported, O3-Na_xMnO_2 delivered a capacity of 185 mAh g^{-1} at 0.1 C in the voltage window of 2.0—3.8 V [21]. But P2-$Na_{0.7}MnO_2$ only showed a reversible capacity of 163 mAh g^{-1} and the capacity was 123.95 mAh g^{-1} after 50 cycles (40 mA g^{-1}, 2.0—4.5 V) [17]. The same O3-type compounds such as $NaFeO_2$, Na_xCoO_2 and Na_xNiO_2 showed a high capacity. However, the layer oxides are found to drive several structural phase transitions: O3-O′

size distribution studies were carried out with field emission scanning electron microscope (FESEM, Hitachi S-4800). The microstructure and element distribution of particle was observed by high resolution transmission electron microscopy and the EDX mapping (JEM-2100F microscope operating at 200 kV). The element valence was determined by X-ray photoelectron spectroscopy (XPS, K-Alpha1063, Japan).

2.2. Electrochemical measurement

Positive electrodes were prepared by mixing 10 wt % of Acetylene black, 80 wt % of active material and 10 wt % of PVDF in N-methyl-2-pyrrolidone (NMP) and coating the slurry on Al foil. The active material mass loading in the electrodes was about 2 mg cm^{-2}. The button cells were assembled in an argon filled glovebox. Sodium metal was used as counter and reference electrodes, and the metal sodium was cut from sodium chunks (99.8%, Aladdin) and then made into sodium tablets. The positive electrodes separated from the negative electrode 3 sheets of glass fiber disks which are soaked with a 1 M solution of $NaClO_4$ in an ethylene carbonate (EC)/Propylene carbonate (PC) mixture (1/1 v/v). Cells were cycled galvanostatically at different constant current rates (theoretical capacity = 240 mAh g^{-1}, 1 C = 240 mA g^{-1}) between 2.0 and 4.2 V in Neware battery tester (BTS-XWJ-6.44S-00052 Neware, Shenzhen, China). Cyclic voltammetry (CV) tests were performed at a scan rate of 0.1 mV s^{-1} between 2.0 and 4.2 V (vs Na^+/Na). CV were conducted using an electrochemical workstation (CHI660e Chenhua, China) The EIS was also recorded using the CHI over the frequency range from 10 mHz to 100 kHz, while the disturbance amplitude was 5 mV. All the electrochemical measurements were carried out at 25 °C.

3. Results and discussion

The elemental composition of the material was deduced from ICP-OES analysis result. The relative elements ratio of Na, Mn, Co and Ni was Na: Mn: Co: Ni = 1.03: 0.674: 0.173: 0.157 for NaMCN. The sodium and transition metal ratio of the material is in a good consistent with designed sample. Hence, the material can be described as $NaMn_{2/3}Co_{1/6}Ni_{1/6}O_2$.

The results of powder X-ray diffraction (XRD) of NaNMC are shown in Fig. 2. The Rietveld refinement is calculated on the Na_xCoO_2 model structure with rhombohedral symmetry (*R*-3*m* space group PDF No: 01-070-2030). As shown in Fig. 2 the observed pattern is consistent with the calculated pattern. The impurity peaks corresponding to sodium salts and manganese, cobalt or nickel oxides are not observed. The parameters R_p, R_{wp}, and χ^2, where R_p and R_{wp} are the profile and weighted profile R-factors, and χ^2 is the goodness-of-fit parameter, are 4.13%, 5.37%, and 4.65%, respectively. The calculated lattice parameters are a = b = 2.8528 (5) Å and c = 16.7676 (4) Å, respectively. The ellipse region identified in the picture shows a very weak peak which cannot match the calculated theoretical peak position. By comparison, the weak peak may originate from the P3 phase (*R*-3*m* space group). The formation of P3 phase is due to a long time high temperature sintering, but the proportion of P3 phase is too small to affect the electrochemical performance of the NaMCN. In general, the detected crystal information is well matched with the ideal O3-type layered structure model. The XRD pattern confirms the materials with the space group *R*-3*m*.

The morphologies of the as-prepared precursor and NaMCN are shown in Fig. 3(a) and (b). As shown in Fig. 3(a), the size of precursor powder is average about 1 μm with regular spherical morphology. Each spherical particle is made up of primary nanoparticles of similar size. The primary nanoparticles are the same as the flake shape of brucite and the particles size is about 200 nm. As shown in Fig. 3(b), the NaMCN sample also shows a uniform spherical morphology. However, the particles show a slightly agglomeration and the particle size slightly grows up. In addition, the pore structure on the surface of the NaMCN sample is disappeared and the surface and edges of NaMCN become smooth, which will improve the tap density of the material. The structure of NaMCN is further characterized by transmission electron microscope (TEM) in Fig. 3(c). The results obtained from TEM correlate well with SEM results. Fig. 3(d) and (e) show the fast Fourier transform (FFT) pattern and representative high-resolution TEM image. Fig. 3(e) shows the crystal lattice fringe spacing is 2.47 Å,

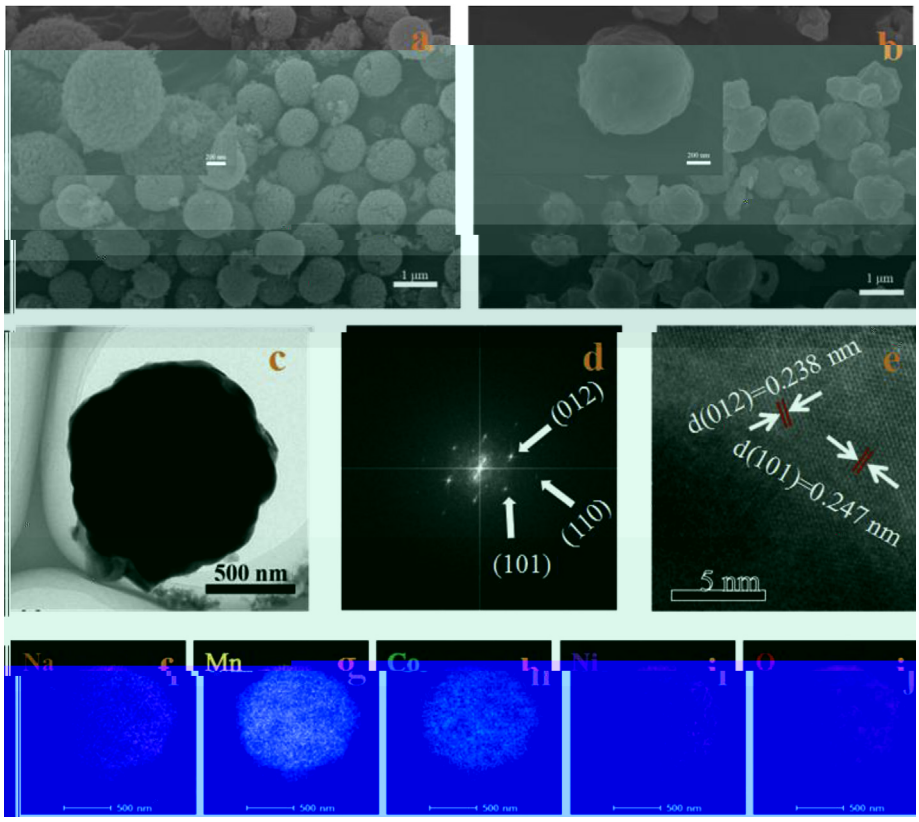

Fig. 3. (a) SEM image of $Mn_2Co_{0.5}Ni_{0.5}O_2$, (b) SEM image of NaMCN cathode material, (c) TEM image of NaMCN, (d) HRTEM image of NaMCN and (e) the fast Fourier transform pattern, (f–j) distribution of elements in the NaMCN.

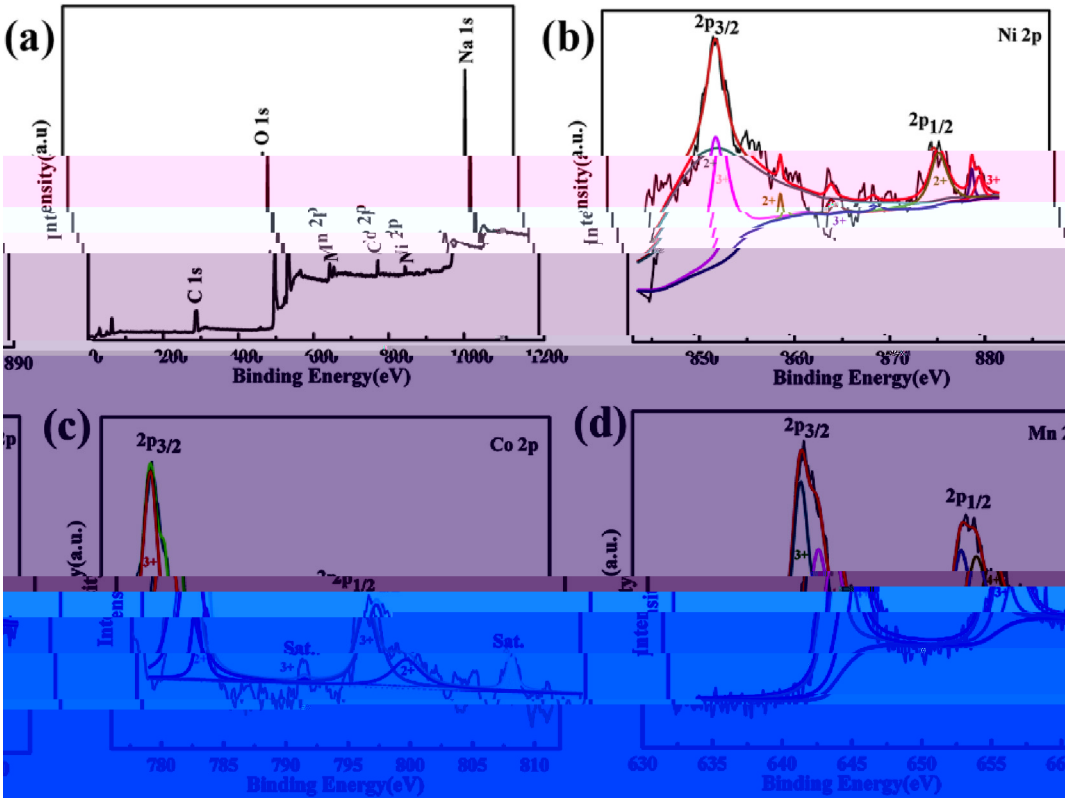

Fig. 4. XPS spectra of (a) survey spectrum, (b) Ni 2p, (c) Co 2p and (d) Mn 2p for NaMCN.

there are a couple of less obvious peaks at 644 and 653.8 eV are observed and these are corresponds to Mn (III) cation [28].

The existence of Mn^{3+} and Ni^{3+} in transition-metal ions is attributed to the electron transfer between Ni^{2+} and Mn^{4+} ion pairs leading to valency-degeneracy by the dynamic equilibrium reported by Shaju et al. [29]. The XPS result proves that the majority oxidation states are in 2 + and 4 + of Ni and Mn ions in NaMCN. Moreover, Ni^{3+} and Mn^{3+} ions in the lattice may be caused by valence degradation. The Ni^{2+} and Co^{3+} cations could be assigned to the electrochemically active transition metal ions which undergo redox transitions during Na^{+} intercalation/deintercalation. While Mn^{4+} cations are assigned to electrochemically inactive and they are considered to enhance the stability of the sample material structure [30,31]. Thus, the above result indicates that NaMCN has a stable structure and good electrochemical activity.

The electrochemical performance of NaNMC is tested by assembling sodium half cells. The electrochemical properties of NaMCN sample is first investigated by CV. Fig. 5(a) shows the CV curves of the NaMCN electrode between 2.0 and 4.2 V versus Na^{+}/Na at the scan rate of 0.1 mV s^{-1}. The half cells show an open circuit

rate performances of NaMCN could be efficiently improved.

Fig. 5(b) shows the charge and discharge performance of NaMCN as a cathode material. As shown in Fig. 5(b), when cycled at 0.1 C, the NaMCN sample exhibits the initial charge and discharge capacities of 157.1 and 153.6 mAh g^{-1}, respectively as well as the coulombic efficiency of 97.3%. The initial discharge specific capacity is higher than that of $NaMn_{1/3}Co_{1/3}Ni_{1/3}O_2$, which has been reported by Sathiya et al. [13]. Furthermore, it can be seen from corresponding CV curves that there is no obvious charge and discharge platform at 2.3 V and 3.5 V, so this further demonstrates that there is no O3-P3 phase transformation. The solution reaction during Na extraction and insertion creates the sloping region [35]. The discharge capacity for the 2nd, 3rd, 50^{th} and 100^{th} are 153.2, 151.7, 141.2 and 124.9 mAh g^{-1}, respectively. According the charge profile, the capacity fading only derives from high voltage (>3.25 V), which is may be assigned to the catalytic decomposition of Na-based electrolyte and the structure irreversibility of the NaMCN at high voltage.

Fig. 5(c) illustrates a C-rate test, the current densities from 0.1 C to 1 C within 2.0−4.2 V. When coming back the current density of 0.1 C again, the discharge capacity could be almost recovered to 150 mAh g^{-1}, which proves that NaMCN possesses a good rate performance and excellent cyclic stability. The structure of NaMCN is stable because special spherical shape can withstand the changes of high stress during Na intercalation/deintercalation processes at high current densities. Compared with the same type of materials [12]. NaMCN sample shows an improved rate performance, indicating an improved kinetics. Such excellent cycling and rate performance suggest that O3-NaMCN will be a promising cathode material for SIBs. The selected charge/discharge curves at the 0.1, 0.2, 0.5 and 1 C rates of NaMCN are presented in Fig. 5(d). The reversible capacities are 153.6, 135.9, 115.6 and 91.6 mAh g^{-1}, respectively. In addition, when the current density increases, even though more obvious electrode polarization of NaMCN sample is observed, the polarization is the smallest compared with the same type of electrode materials [36]. The coulombic efficiencies are close to 100% during cycling at 0.2, 0.5 and 1 C, which indicates that the insertion process is not limited. However, the electrode polarization presents a slight growth at different rates, which indicates that the resistance of Na^+ diffusion increases at high current density.

The cycling performances of NaMCN at 0.1 C and 0.5 C are shown in Fig. 5(e). When the NaMCN sample cycles at 0.1 C, the electrode

process. The $NaNaMn_{2/3}Co_{1/6}Ni_{1/6}O_2$ exhibited an initial specific discharge capacity of 153 mAh g^{-1} at 0.1 C with capacity retention of 81.7% after 100 cycles. A remarkable rate performance is obtained after 50 cycles at 0.5 C with good capacity retention of 92.3%. It can be considered that a part of Co^{3+} and Ni^{3+} in the TM layers could improve structure stability during Na^+ intercalation/deintercalation processes. Moreover, the introduction of Co^{3+} can reduce the mixed cation occupying, increase the diffusion rate of Na^+, enhance the conductivity, and improve cycle and rate performance of sample. In the same time, NaMCN could suppress the occurrence of multi-phase transitions, and there is a wide voltage window (2.0−4.2 V). As a result, $NaMn_{2/3}Co_{1/6}Ni_{1/6}O_2$ will be a promising high-performance cathode material for the application of SIBs.

Acknowledgement

This work is supported financially by the National Natural Science Foundation of China under project (No. 51272221), the Key Project of Strategic New Industry of Hunan Province under project (No. 2016GK4005 and 2016GK4030).

References

[1]